Targeting of Pancreatic Glia in Type 1 Diabetes

Hubert Tsui,[1] Yin Chan,[1] Lan Tang, [1] Shawn Winer,[1] Roy K. Cheung,[1] Geoffrey Paltser,[1] Thirumahal Selvanantham,[1] Alisha R. Elford,[3] James R. Ellis,[1] Dorothy J. Becker,[2] Pamela S. Ohashi,[3] and Hans-Michael Dosch[1]

OBJECTIVE—Type 1 diabetes reflects autoimmune destruction of β-cells and peri-islet Schwann cells (pSCs), but the mechanisms of pSC death and the T-cell epitopes involved remain unclear.

RESEARCH DESIGN AND METHODS—Primary pSC cultures were generated and used as targets in cytotoxic T-lymphocyte (CTL) assays in NOD mice. Cognate interaction between pSC and $CD8^+$ T-cells was assessed by transgenic restoration of β2-microglobulin (β2m) to pSC in NOD.$\beta2m^{-/-}$ congenics. I-A^{g7} and K^d epitopes in the pSC antigen glial fibrillary acidic protein (GFAP) were identified by peptide mapping or algorithms, respectively, and the latter tested by immunotherapy.

RESULTS—pSC cultures did not express major histocompatibility complex (MHC) class II and were lysed by ex vivo CTLs from diabetic NOD mice. In vivo, restoration of MHC class I in GFAP-β2m transgenics significantly accelerated adoptively transferred diabetes. Target epitopes in the pSC autoantigen GFAP were mapped to residues 79–87 and 253–261 for K^d and 96–110, 116–130, and 216–230 for I-A^{g7}. These peptides were recognized spontaneously in NOD spleens as early as 2.5 weeks of age, with proliferative responses peaking around weaning and detectable lifelong. Several were also recognized by T-cells from new-onset type 1 diabetic patients. NOD mouse immunotherapy at 8 weeks with the $CD8^+$ T-cell epitope, GFAP 79–87 but not 253–261, significantly inhibited type 1 diabetes and was associated with reduced γ-interferon production to whole protein GFAP.

CONCLUSIONS—Collectively, these findings elucidate a role for pSC-specific $CD8^+$ T-cells in islet inflammation and type 1 diabetes pathogenesis, further supporting neuronal involvement in β-cell demise. ***Diabetes*** **57:918–928, 2008**

From the [1]Department of Pediatrics, Immunology and Genetics, the Research Institute, the Hospital for Sick Children, University of Toronto, Toronto, Ontario, Canada; and the [2]Department of Pediatrics, Children's Hospital and University of Pittsburgh, Pittsburgh, Pennsylvania; and the [3]Departments of Medical Biophysics and Immunology, Campbell Family Institute for Breast Cancer Research, Ontario Cancer Institute, University Health Network, University of Toronto, Toronto, Ontario, Canada.

Address correspondence and reprint requests to Hans-Michael Dosch, The Hospital for Sick Children, 555 University Ave., 10th Floor Elm Wing, Rm. 10126, Toronto, Ontario, M5G 1X8, Canada. E-mail: hmdosch@sickkids.ca.

Received for publication 21 February 2007 and accepted in revised form 9 January 2008.

Published ahead of print at http://diabetes.diabetesjournals.org on 25 January 2007. DOI: 10.2337/db07-0226.

Additional information for this article can be found in an online appendix at http://dx.doi.org/10.2337/db07-0226.

AIM, adoptive immunotherapy media; β2m, β2-microglobulin; CTL, cytotoxic T-lymphocyte; FDR, first-degree relative; GFAP, glial fibrillary acidic protein; IFA, incomplete Freund's adjuvant; IFN-γ, γ-interferon; IL, interleukin; MHC, major histocompatibility complex; pSC, peri-islet Schwann cell; SI, stimulation index; TCR, T-cell receptor.

Destruction of insulin-producing pancreatic β-cells by T-lymphocytes results in type 1 diabetes (1). In humans and the nonobese diabetic (NOD) mouse, both genetic (e.g., major histocompatibility complex [MHC]) and environmental (e.g., diet and infection) factors influence development of overt disease. Although the precise mechanisms remain unclear, evidence suggests that the early stages of disease development involve the draining pancreatic lymph nodes (2).

(Pro)insulin, GAD65, insulinoma-associated antigen 2, islet-specific glucose-6-phosphatase catalytic subunit–related protein, HSP60, and islet cell antigen 69 kDa are autoantigens in type 1 diabetes (3). Many of these antigens are not expressed solely in β-cells but are predominant in systemic neuro-endocrine tissues. Why widely expressed antigens are involved in local islet inflammation is not clear, although dysfunctional sensory neurons contribute (4). Previously, we reported that autoimmune targeting in type 1 diabetic patients and NOD mice is similar to that observed in those with multiple sclerosis, with significantly elevated risks of developing both diseases (5,6). While the NOD mouse does not spontaneously develop nervous system disease, its propensity toward neuronal pathology becomes manifest with adjuvant (5), B7-2 deficiency (7), or interleukin (IL)-2 blockade (8).

In examining pancreatic nervous system tissue elements, we found that the glial sheath composed of peri-islet Schwann cells (pSC) is destroyed spontaneously during pre-diabetes in NOD mice and likely pre-diabetic humans (9). This destruction is associated with pSC-reactive T-cells and autoantibodies targeting glial fibrillary acidic protein (GFAP), a cytoskeletal protein predominantly expressed in Schwann cells and astrocytes (10). A full understanding of pSC and GFAP in pre-diabetes progression is lacking (11), and it is unclear whether pSC death reflects collateral damage in a proinflammatory milieu or cognate autoimmune targeting which would break the β-cell specificity of type 1 diabetes.

Here, we report the cognate targeting of pSC both in vitro and in vivo and refine the autoimmune GFAP T-cell response to K^d and I-A^{g7} epitopes. Several NOD target epitopes were also found to be prominent targets in children with type 1 diabetes. Together, these findings assign pSC a distinct role in type 1 diabetes pathogenesis, with $CD8^+$ T-cell targeting of GFAP participating in type 1 diabetes progression.

RESEARCH DESIGN AND METHODS

NOD/LtJ, NOD.129P2(B6)-$B2m^{tm1Unc}$/J (NOD.$\beta2m^{-/-}$), and C57BL/6J (B6) mice were purchased from The Jackson Laboratory (Bar Harbor, ME). NOD AI4 T-cell receptor (TCR) transgenics were donated by Dr. David Serreze (The Jackson Laboratory). Mice were maintained in our conventional facility under approved protocols. Glucosuria was used to screen for diabetes (Diastix;

Bayer, Toronto, ON, Canada) and confirmed by blood glucose measurements (>13.8 mmol/l) (OneTouch Ultrasmart; Lifescan Canada, Burnaby, BC, Canada).

Transgenic mice. A GFAP promoter expression cassette was donated by Dr. M. Brenner (12). NOD β2-microglobulin (β2m) cDNA was generated by RT-PCR from spleen using β2mBamF 5′-CGCGGATCCATGGCTCGCTCGGTG-3′ and β2mBamR 5′-CGCGGATCCTCACATGTCTCGATC-3′). Six founder mice were generated after ~1 pL injection into hyperovulated, fertilized NOD ova, crossed to NOD.β2m$^{-/-}$ and screened using the genotyping protocol B2m^{tm1Unc} (The Jackson Laboratories). Western blots used goat α-β2m (Santa Cruz Biotechnology, Santa Cruz, CA) and mouse α-goat horseradish peroxidase (The Jackson Laboratory).

Adoptive transfer. Splenocytes (10^7) from pooled spontaneously diabetic NOD females were injected intravenously in 100 μl PBS to NOD males, NOD.β2m$^{-/-}$ females, or GFAP-β2m Tg female recipients irradiated 650 cGy, 24 h before transfer.

T-cell proliferation assay. Mouse spleens were dissociated and red cells lysed by hypotonic shock. A total of 4.5×10^5 splenocytes/well were cultured in adoptive immunotherapy media (AIM)-V media (Gibco) plus 5% fetal bovine serum (Gibco) containing antigen in 96-well flat-bottom plates (BD). After 72 h, cultures were pulsed (1 μCi [3H]thymidine/18 h) and counted by liquid scintillation. Supernatants were collected after 48 h for cytokine enzyme-linked immunosorbent assay following the manufacturer's instructions (BD). Patients with new-onset type 1 diabetes or first-degree relatives (FDRs) of type 1 diabetic patients were invited to participate under approved protocols and after signing informed consent at the Pittsburgh Children's Hospital. Heparinized peripheral blood was sent to the Toronto assay lab (H.-M.D) by overnight courier, and mononuclear cells were prepared and cultured as described (9). To normalize results from human and mouse experiments, some data are presented as stimulation index (SI) (SI = antigen cpm/media cpm). K^d inhibition used the SF1–1.1 monoclonal antibody (BD).

Flow cytometry. Splenocytes were stained with CD3-FITC, CD8-APC, and CD4-PE (BD Pharmingen, Mississauga, ON, Canada). Live events were collected based on forward-and side-scatter profiles on a FACScan flow cytometer (BD) and analyzed using FlowJo software (Stanford University).

GFAP immunization. Eight-week-old NOD females were immunized with 5 μg GFAP, emulsified in incomplete Freund's adjuvant (IFA) (Sigma) in the hind footpads (50 μl/foot), and boosted intraperitoneally 10 days later with 5 μg GFAP IFA. Spleens were harvested 10 days after the seecond injection for in vitro T-cell proliferation assay.

Antigens. Overlapping 15-mer peptides with an offset of five amino acids were purchased from Mimotope (Clayton, Australia). The mus musculus sequence of GFAP (418 amino acids) from the NCBI protein database (Accession NP_034407) was used (13). Peptides were dissolved in PBS (Gibco) and for insoluble peptides, DMSO or acetic acid was added. GFAP 79–87, 96–110, 116–130, 216–230 and 253–261 were synthesized at >90% purity (Alpha Diagnostics International, San Antonio, TX). Other antigens included human GFAP (Calbiochem, San Diego, CA) and ovalbumin (Sigma). Human T-cell assay antigens have previously been described (5).

Histology. Frozen pancreas sections were fixed in 1% paraformaldehyde and blocked with 5% normal donkey serum (Jackson ImmunoResearch, Westgrove, PA). Primary antibodies: rabbit α-GFAP (Signet Pathology Systems, Dedham, MA), guinea pig α-insulin (DAKO, Carpinteria, CA), goat α-CD3 (Santa Cruz), goat α-glucagon (Santa Cruz), mouse α-β2m (Santa Cruz), biotinylated α-I-A^b (BD), and mouse anti-CD8-biotin (BD). Secondary reagents included donkey α-rabbit fluorescein isothiocyanate, donkey α-goat Cy5, donkey α–guinea pig Cy5, donkey α-goat Cy5 (Jackson ImmunoResearch), donkey α-goat AlexaFluor 546, Strepavidin AlexaFluor 633 (Molecular Probes, Eugene, OR), and propidium iodide or DAPI (Sigma). Immunofluorescence was visualized by confocal microscopy (Zeiss).

Islet isolation and pSC culture. Islets were isolated using standard protocols (14). For pSC cultures, standard islet isolations were performed, but islets were cultured in laminin-coated dishes (Sigma) using Dulbecco's modified Eagle's medium (DMEM) with 2.5% fetal bovine serum, 0.2% bovine pituitary extract, and forskolin (Sigma) (15). Media were changed twice weekly. At ~80% confluency, islets were handpicked from the culture followed by treatment with 10 mmol/l alloxan (Sigma) for 15 min consecutively over 2 days. At confluency, media was changed to 2.7 ml DMEM + 0.3 ml dissociation medium (10 ml DMEM + 250 mg Dispase [Gibco] and 50 mg collagenase type I [Sigma]) and incubated for 3 h at 37°C. A flame-narrowed Pasteur pipette was used to triturate the cells and, following two washes, seeded for cytotoxic T-lymphocyte (CTL) assay. Islets and pSC cultures were derived from either NOD.scid or 4-week-old B6 or NOD females.

Cytotoxicity assay. Islets or pSC were seeded in 96-well flat-bottom plates (BD) at 4×10^4 cells/well in AIM-V. pSCs were stimulated for 48 h with 100 units/ml recombinant mouse IFN-γ (Sigma) before 1 h labeling with ^{51}Cr. Splenocytes or CD8$^+$ T-cells (EasySep; Stem Cell Technologies, Vancouver, BC, Canada) in AIM-V were added at various effector:target cell ratios. After 8 h at 37°C, 70 μl supernatant was counted. RMA-S K^d targets were a gift of P. Santamaria (Calgary, AB, Canada) and used as previously described (16). RMA-S K^d cells were pulsed with 5 μg/ml peptide. Specific lysis was calculated as follows: (cpm sample release − cpm spontaneous release)/(cpm maximal release − cpm spontaneous release).

RESULTS

Generation of peri-islet Schwann cell cultures. To date, pSC destruction has been inferred from immunohistochemistry of pancreas sections of NOD mice (9). To directly visualize pSC-directed autoimmune targeting, we generated pSC lines in vitro. Primary pSC cultures were derived from freshly isolated islets (Fig. 1*A*) by growth in selective media (15). Fresh islets contain the expected distribution of endocrine cells with insulin-stained β-cells (blue) in the center surrounded by glucagon-stained α-cells (red) (Fig. 1*B*). Only sparse numbers of islet-adherent GFAP$^+$ pSC survive the stress of collagenase digestion and isolation procedures, which strip the pSC envelope (Fig. 1*C*). Variations in digestion time affected pSC yields dramatically. However, over the ensuing 3- to 5-week culture period, pSC proliferate extensively, generating lawns of GFAP$^+$ glial cells (Fig. 1*D–F*). Growing pSCs generate a network and actively envelope islets, suggestive of a strong tropism between islets and pSC (Fig. 1*D* and *E*) (17). In the cultures used for subsequent experiments, contaminating islets were removed manually, followed by two consecutive treatments with alloxan. Remaining cells were >94% pSC as assessed by flow cytometry for p75 nerve growth factor receptor expression (data not shown) (15) and immunofluorescent staining for GFAP and insulin, with glucagon-negative, fibroblast-like cells as the minor contaminant.

T-Cell targeting of pSC in vitro. GFAP-stained pSC cultures exhibited dendritic morphology reminiscent of astrocytes (Fig. 1*G*). To determine whether pSC expressed MHC class II, pSC cultures were treated with IFN-γ for 24 h and then observed by immunohistochemistry. MHC class II was undetectable in pSC cultures as expected (18), with added antigen-presenting cells serving as positive controls (Fig. 1*H*).

As NOD T-cells recognize pSC auto-antigens such as GFAP in proliferation assays (9), we asked whether pSC would be killed ex vivo by pSC-reactive T-cell pools. A spontaneous CTL assay using pSC targets was developed, initially with isolated NOD islets (Fig. 1*I*). Purified NOD pSC cultures were then generated and treated with IFN-γ (to upregulate MHC class I) before labeling and incubation with fresh splenocytes or negatively selected CD8$^+$ T-cells from spontaneously diabetic NOD mice. As shown in Fig. 1*J* and *L*, ex vivo CTL activity toward IFN-γ treated pSC was detectable without prior CTL activation in culture or exogenous peptide pulsing. pSC lysis was significantly higher in the NOD ($P < 0.03$) than in the B6 control assays (Fig. 1*J* and *L*), although some background B6 killing was observed.

CTL-mediated lysis in this system appears to be dependent on MHC class I, as killing was negligible with NOD.β2m$^{-/-}$-derived pSC (Fig. 1*K*). That pSC destruction may be predominantly CD8$^+$ T-cell dependent was corroborated by immunohistochemistry of spontaneously diabetic NOD BDC2.5 T-cell receptor transgenics. Pancreas sections in this CD4$^+$ T-cell–mediated diabetes model revealed intact pSC mantles surrounding remaining α-cells (Fig. S1 [available in an online appendix at http://dx.doi.

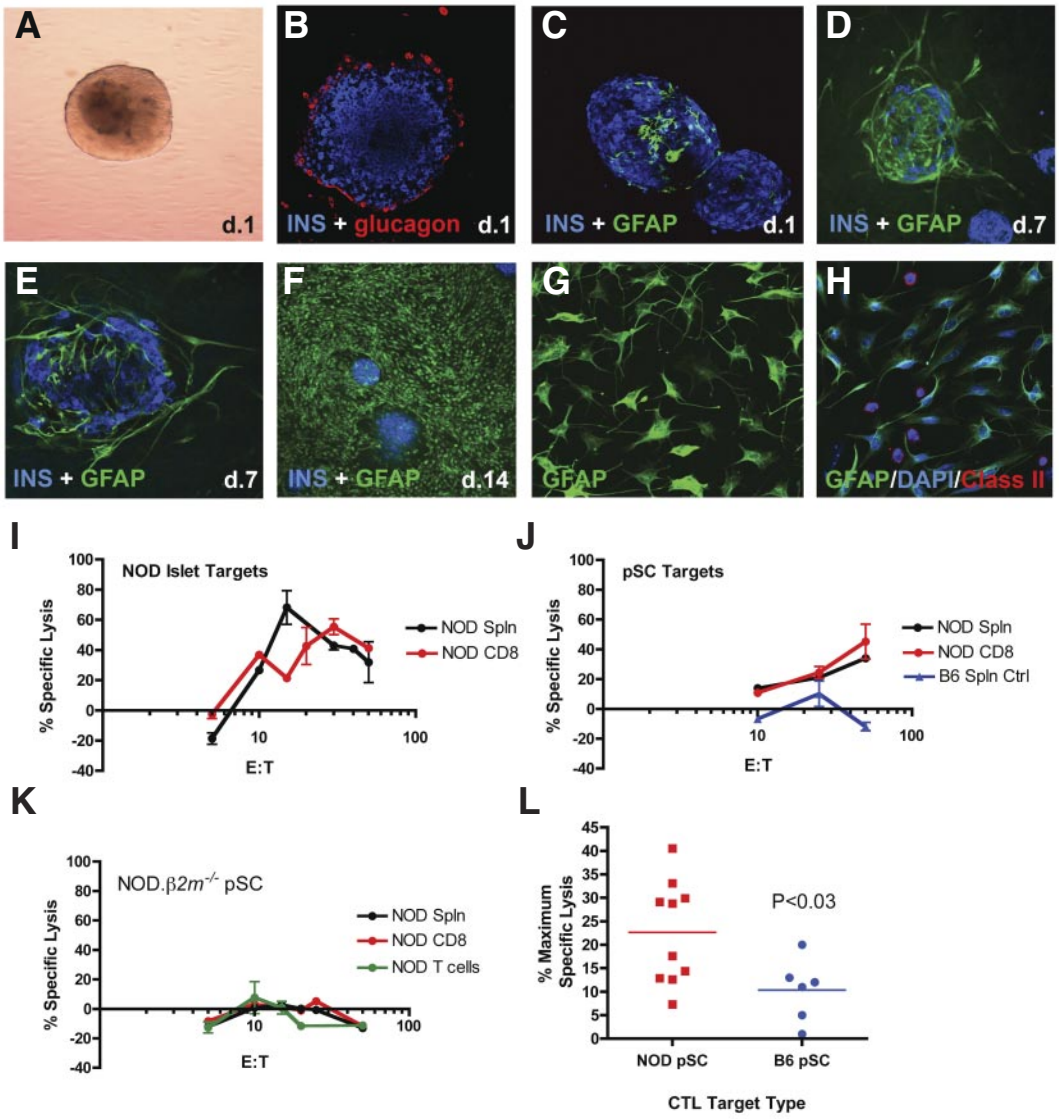

FIG. 1. Generation of pSC in vitro and targeting by ex vivo CTL. *A*: Light microscopy of a freshly isolated islet (100×). *B* and *C*: Islet architecture after 24 h of culture. Islets stained with insulin (blue) and glucagon (red) or GFAP (green), 200×. *D–F*: Schwann cell growth media expands pSC, enveloping β-cells over 2–3 weeks (GFAP, green; insulin, blue; 200×). *G*: Purified pSC cultures show astrocyte-like dendritic morphology (400×; GFAP, green). *H*: IFN-γ–treated pSC cultures do not express MHC class II (red). GFAP (green); nuclear DAPI stain (blue). Monocytes served as positive control. Whole NOD islets (*I*), or cultured purified pSC (*J–L*) were exposed to IFN-γ before incubation with splenocytes (Spln) or negatively selected splenic CD8$^+$ T-cells from diabetic NOD donors. *I*: ^{51}Cr release assay with cultured islets. *J*: Representative CTL assay with NOD spleen cells or CD8$^+$ T-cell effectors and purified NOD pSC targets. Control B6 spleen cells assayed with B6-purified pSC shown in blue. *K*: Representative CTL assay using NOD.β2m$^{-/-}$ pSC targets and NOD Spln, purified T-cells, or CD8 T-cell effectors. *L:* Pooled CTL assay data comparing NOD vs. B6 maximum pSC lysis, $P < 0.03$ by t test. (Please see http://dx.doi.org/10.2337/db07-0226 for a high-quality digital representation of this figure.)

org/10.2337/db07-0226]). Thus, it appears that at least one mechanism of pSC destruction involves cognate CD8$^+$ CTL.

Relevance of pSC destruction in diabetes progression. To investigate the in vivo relevance of CTL reactivity toward pSC, we generated transgenic mice that limited CTL–β-cell contact to pSC. NOD.β2m$^{-/-}$ mice do not develop spontaneous diabetes but do develop peri-islet T-cell aggregates >30 weeks of age without pSC damage (Fig. S2), further supporting the importance of CD8$^+$ T-cells in pSC targeting. Importantly, NOD.β2m$^{-/-}$ mice can become hyperglycemic several months after adoptive transfer with wild-type splenocytes from diabetic donors (19–21). To selectively restore β2m expression in Schwann cells, we used a well-characterized GFAP promoter (12) to drive NOD β2m expression (Fig. 2*A*). Injection of the transgene into fertilized NOD eggs yielded multiple founder lines (Fig. 2*B*), which were bred to NOD.β2m$^{-/-}$ congenic stock (Fig. 2*C*). Homozygous β2m$^{-/-}$ transgenics were then analyzed for β2m expression by Western blot and immunostaining in brain and pancreas (Fig. 2*D–F*).

Based on good breeding and nonleaky transgene expression, transgenic lines 9 and 14 were selected for further study, generating similar results. As expected, endogenous CD8$^+$ T-cells were absent in spleen cells of GFAP-β2m transgenics (Fig. 3*A–C*), and they resisted development of spontaneous diabetes (Fig. 3*D*). In adoptive transfer experiments (22), splenocytes from diabetic females transferred hyperglycemia to irradiated wild-type NOD males

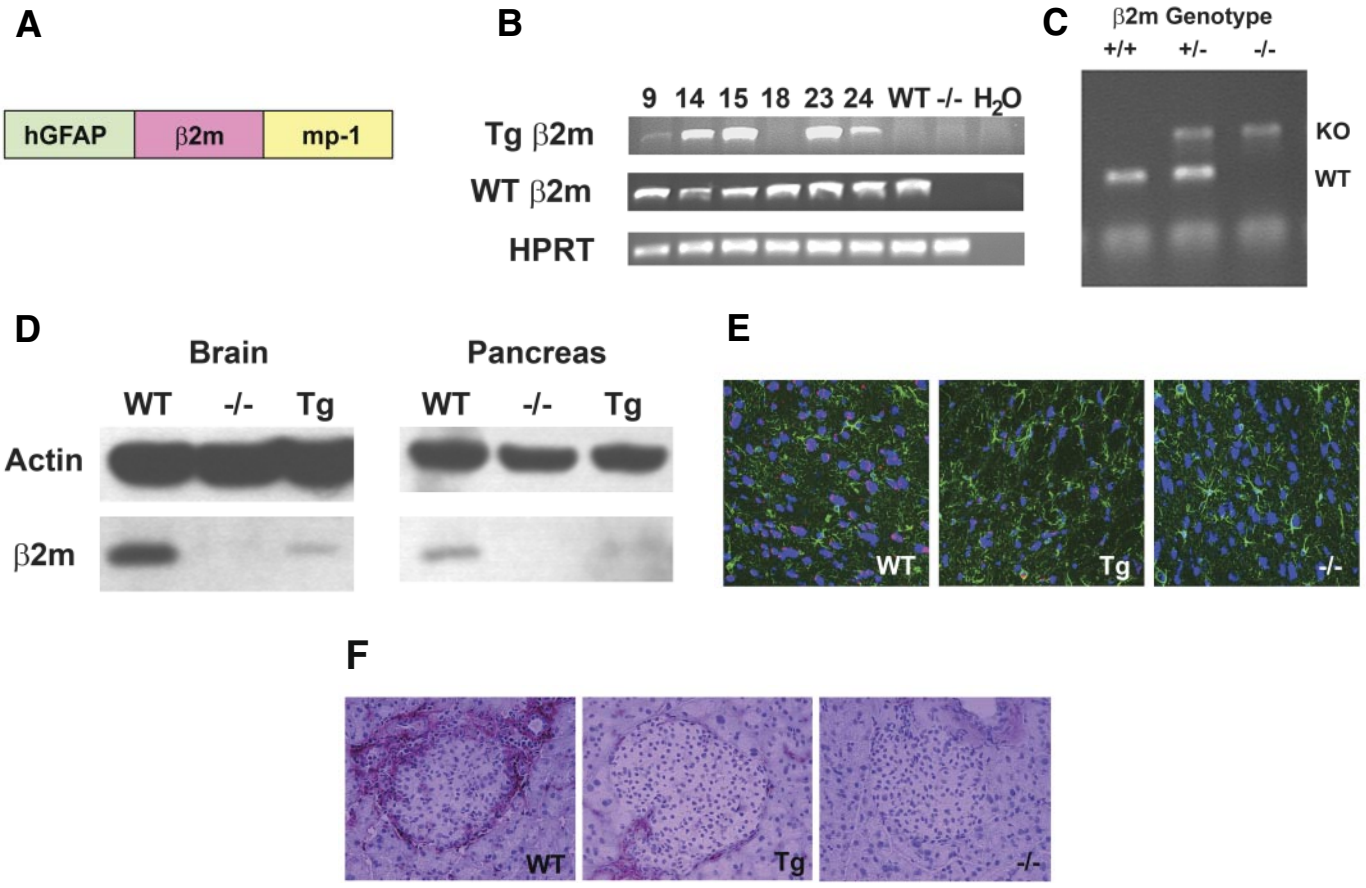

FIG. 2. Transgenic restoration of β2m expression in glia of NOD.β2m$^{-/-}$ mice. *A*: Transgene schematic. NOD β2m cDNA was cloned into a human GFAP promoter expression cassette. *B*: Six founder lines were generated directly in NOD fertilized eggs and five confirmed by RT-PCR from brain cDNA. Transgenic (lines 9 and 14) mice were backcrossed to NOD.β2m$^{-/-}$ and homozygous β2m null mice (*C*), and analyzed for protein expression in brain and pancreas by Western blot (*D*) and histology (*E* and *F*). *E*: Brain sections from wild-type (WT) NOD, transgenic GFAP-β2m line 9 (Tg), and NOD.β2m$^{-/-}$ (-/-) mice are depicted (GFAP, green; β2m, red; PI, blue; 200×. Histological detection of β2m appears pink in astrocytes. *F*: Islets of wild-type, transgenic GFAP-β2m line 9, and NOD.β2m$^{-/-}$ mice with β2m horseradish peroxidase staining (brown) counterstained with hematoxylin; 200×. (Please see http://dx.doi.org/10.2337/db07-0226 for a high-quality digital representation of this figure.)

within 5 weeks, while nontransgenic NOD.β2m$^{-/-}$ mice were very slow to develop disease and in only a few animals (Fig. 3*E*). In contrast, GFAP-β2m mice developed diabetes at a significantly faster rate and higher incidence than nontransgenic littermates ($P = 0.0016$, log-rank test). Both founders gave similar results. Hyperglycemia in transgenic mice was associated with progressive autoimmune insulitis and destruction of pSC (Fig. 3*F*–*I*), with increased retention/recruitment of CD8$^+$ T-cells to the islet locale (Fig. S3).

To ensure that disease acceleration was not due to MHC class I stabilization on β-cells from soluble β2m possibly derived from pSC, we employed a β-cell–specific TCR transgenic system. The AI4 TCR recognizes dystrophia myotonica kinase (23) and induces rapid spontaneous diabetes by 4 weeks of age (24). Compared with spontaneous NOD diabetes, AI4-mediated hyperglycemia occurs with only minor pSC disruption (Fig. 4*A* and *B*). Using a robust AI4 adoptive transfer protocol (25), rapid disease developed in wild-type recipients but not GFAP-β2m transgenics or NOD.β2m$^{-/-}$ controls, excluding biologically relevant amounts of MHC class I stabilization on β-cells in our GFAP-β2m model (Fig. 4*C*).

Characterization of I-A^{g7} and K^d GFAP epitopes. To further characterize pSC autoimmunity, we sought to define NOD GFAP epitopes. The NOD MHC haplotype includes the common MHC class I alleles K^d and D^b and the rare MHC class II allele I-A^{g7} and is I-E null (1). While search algorithms exist for the K^d and D^b alleles, none are available for the unique I-A^{g7}, although preferred peptide-binding motifs have been reported (26,27). To identify MHC class II GFAP epitopes, an overlapping 15-mer peptide map of the entire murine GFAP sequence was synthesized. Proliferative splenic responses to GFAP peptides were measured 10 days following immunization with whole GFAP protein in IFA. Pooled results from 10 individual assays are shown in Fig. S4, with top-responding peptides in Table S1. We selected IFA over CFA to avoid a strong TLR-mediated immune response and more closely mimic autoimmune targeting conditions inherent in the NOD mouse. The results presented here focus on epitope mapping with IFA. Complete Freund's adjuvant results yielded an alternate peptide (GFAP106–120), summarized in Fig. S5 and Table S2.

From the initial list of GFAP-IFA–generated putative CD4$^+$ T-cell epitopes, peptides were selected that contained preferred I-A^{g7} anchor residues, including large hydrophobic or positively charged residues at P6 and aromatic hydrophobic or positively charged residues at P9 (26,27). Using these criteria, GFAP epitopes with predicted I-A^{g7} binding are listed in Table 1.

For MHC class I epitopes, the BIMAS (BioInformatics and Molecular Analysis Section) (http://thr.cit.nih.gov) and SYFPEITHI (www.syfpeithi.de) matrix-assisted algorithms

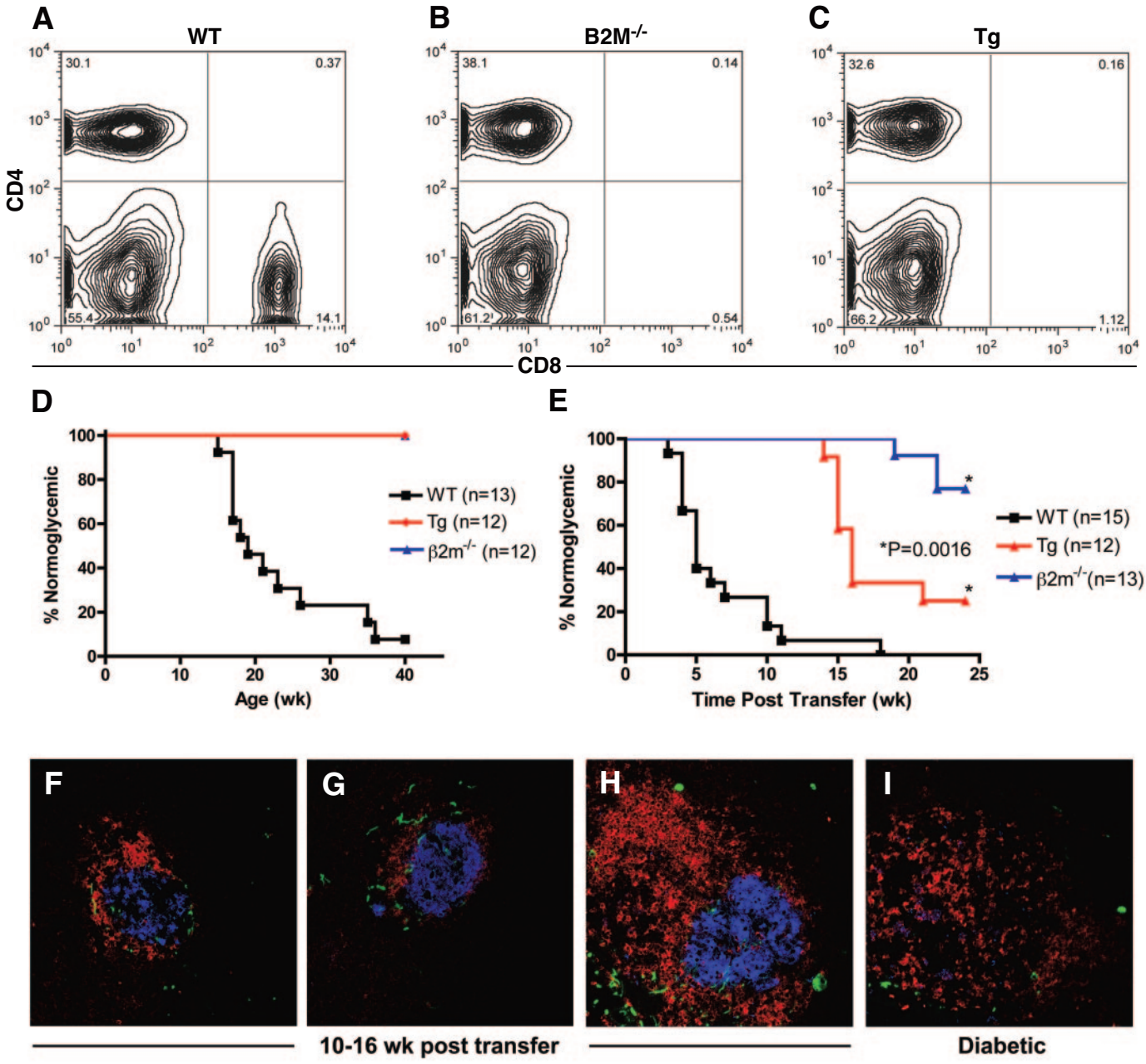

FIG. 3. MHC class I restricted pSC destruction accelerates adoptively transferred diabetes. (*A–C*: CD4 vs. CD8 flow cytometry profiles of splenocytes from wild-type (WT), NOD.β2m$^{-/-}$ and Tg mice, gated on live lymphocytes. *D*: Tg and nontransgenic β2m$^{-/-}$ littermates do not develop spontaneous hyperglycemia. *E*: 8-week-old NOD males, and Tg and β2m$^{-/-}$ females were sublethally irradiated and adoptively transferred with 10^7 diabetic donor splenocytes. Disease kinetics in Tg females were significantly faster than those in β2m$^{-/-}$ mice ($P = 0.0016$, log-rank analysis). *F–I*: Immunofluorescent visualization of pre-diabetes progression in Tg mice 10–16 weeks post transfer and at diabetes onset (*I*) (GFAP, green; insulin, blue; CD3, red); 200×. *A–C* and *F–I*: Tg line 9. *D* and *E*: pooled from Tg lines 9 and 14. (Please see http://dx.doi.org/10.2337/db07-0226 for a high-quality digital representation of this figure.)

were used to predict GFAP peptide sequences for K^d and D^b. BIMAS and SYFPEITHI scores for predicted GFAP K^d epitopes are presented in Table S3. These algorithms did not predict D^b binding peptides.

Spontaneous T-cell reactivity provides strong evidence for immunogenicity, natural processing, and disease relevance. Of the four MHC class II peptides synthesized, 116–130 and 216–230 consistently elicited positive responses in NOD mice, with peak responses occurring after weaning at 4 weeks of age. GFAP96–110 triggered responses to a lesser extent. GFAP321–335 did not respond (not shown). Figure 5 shows cpm data from four individual diabetic mice (Fig. 5*A*, *C*, and *E*) and kinetic results (Fig. 5*B*, *D*, and *F*) expressed as maximum SI). Maximum SI presents the highest proliferation observed irrespective of the peptide concentration (assayed from 5 to 250 μg/ml).

Of the predicted MHC class I epitopes, only GFAP79–87 and 253–261 gave positive T-cell responses (Fig. 5*G–J*). GFAP 112–120, 200–208, and 320–328 remained negative (not shown). The minimum dose at which a proliferative response was observed varied from mouse to mouse, the particular peptide, and their age, likely reflecting stochastic TCR usage and the nonsynchronous disease course.

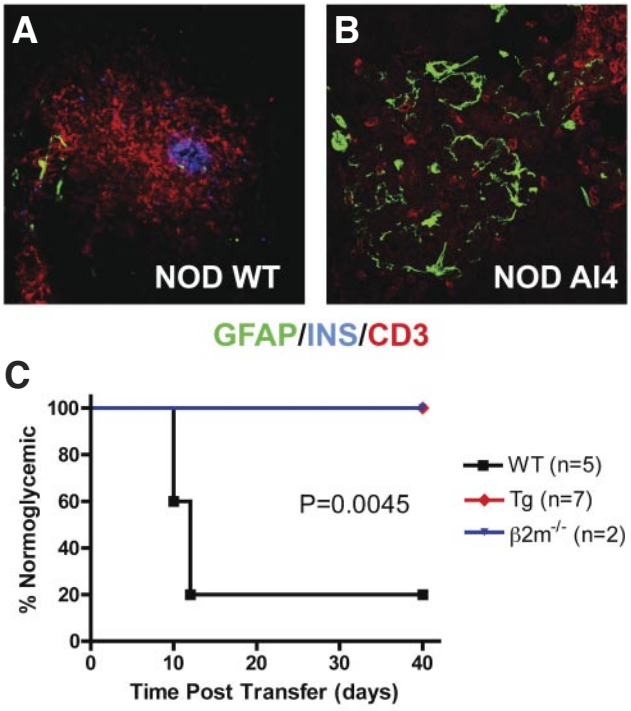

FIG. 4. Accelerated diabetes in GFAP-β2m transgenics is not due to stabilization of β-cell MHC class I. *A* and *B*: Loss of pSC is predominant in spontaneous NOD diabetes (*A*) but less severe in diabetic RAG-1$^{-/-}$ AI4 CD8 TCR transgenics (*B*). GFAP, green; insulin, blue; CD3, red; 400×. *C*: Transfer of 5 × 10^6 AI4 splenocytes to sublethally irradiated wild-type (WT), β2m$^{-/-}$, and Tg mice induces rapid diabetes only in wild-type recipients. Wild type vs. Tg, $P < 0.005$, log-rank analysis. (Please see http://dx.doi.org/10.2337/db07-0226 for a high-quality digital representation of this figure.)

Nevertheless, responses to GFAP epitopes could be detected by 2.5 weeks of age, suggesting that priming and expansion of GFAP reactive T-cell pools occur early along with epitope specificity.

To further confirm the immunogenicity of the putative MHC class II GFAP peptides, 100 μg GFAP 96–110, 116–130, and 216–230 were each emulsified in CFA and recall responses assessed 10 days post–intraperitoneal immunization in 8-week-old NOD mice. All three peptides were immunogenic, as evidenced by boosted recall responses (Fig. S6*a–c*). Interestingly, CFA immunization with this panel of MHC class II GFAP peptides also elevated the low-dose whole protein GFAP response (Fig. S6*d*). This panel of GFAP peptides responds spontaneously in NOD mice but not in the nonautoimmune B6 (Fig. S7).

TABLE 1
Selected epitopes with I-A^{g7} alignment

Peptide	Amino acid position	I-A^{g7} anchor alignment
		6 9
20	96–110	AELNQ**L**RA**K**EPTKLA
		AE**L**NQ**L**RAKEPTKLA
24	116–130	ELRELRLR**L**DQ**L**TAN
		ELREL**R**LR**L**DQLTAN
		ELRE**L**RLR**L**DQLTAN
		ELRE**L**RLRLDQLTAN
44	216–230	QVHVEMDVA**K**PD**L**TA
		QVHVE**M**DV**A**KPDLTA
		QV**H**VE**M**DVAKPDLTA
65	321–335	YQEA**L**AR**L**EEEGQSL
		YQE**A**LARLEEEGQSL

MHC class I specificity of K^d epitopes. To ensure that the MHC class I peptides were indeed CD8$^+$ T-cell specific, 8-week-old NOD females were immunized subcutaneously with GFAP 79–87 or 253–263 in CFA. Five days later, CD8$^+$ T-cells were negatively selected from draining lymph nodes and incubated with peptide-pulsed RMA-S(K^d) targets. GFAP 79–87 and 253–263 immunization generated peptide-specific CTLs (Fig. 6*A*), confirming their MHC class I specificity.

This conclusion was tested by using the monoclonal antibody SF1–1.1 to block K^d in our in vitro proliferation assay. As shown in Fig. 6*B*, K^d inhibition reduced proliferation to GFAP 79–87 and GFAP 253–261, although the effect was more marked in GFAP 79–87. Differing affinities may account for the specific degree of inhibition; nevertheless, it is clear that the GFAP MHC class I peptides are susceptible to K^d inhibition. K^d blockade also partially reduced the response to whole-protein GFAP.

GFAP peptide immunotherapy. We next assessed the disease relevance of MHC class I GFAP epitopes by immunotherapy. 8-week-old NOD females were injected intraperitoneally with 100 μg GFAP 79–87 or 253–261 or vehicle control in IFA. At the dose and route used, GFAP 79–87, but not 253–261, provided significant protection from type 1 diabetes ($P < 0.02$) (Fig. 6*C*). Insulitis in normoglycemic GFAP 79–87–treated animals stalled predominantly at the peri-insulitis stage (data not shown). Intriguingly, diabetes protection was associated with a marked reduction in IFN-γ production to whole-protein GFAP ($P < 0.03$) (Fig. 6*D*, *right side*) despite equivalent proliferative responses in GFAP 79–87 and GFAP 253–261–immunized mice (Fig. 6*D*, *left side*). No differences in IL-10 production or recall responses to the peptides were observed at the end point (not shown); however, GFAP79–87–immunized mice exhibited divergent proliferative responses to whole GFAP and GFAP 216–230 at 10 days posttreatment (Fig. S8). No shifts in peptide responses were observed in GFAP253–261–immunized mice. Alterations in specific GFAP reactive T-cell pools may be responsible for the disease protection; however, the exact mechanism will require further investigation. Nevertheless, immunotherapy with a MHC class I GFAP peptide was capable of modifying diabetes, fulfilling our test of disease relevance.

Human responses to GFAP peptides. Independently, the Nepom group has recently identified human MHC class I GFAP epitopes for HLA-A*0201 (28). Though we used the NOD mouse to identify class I and II restricted GFAP epitopes, the I-A^{g7} MHC class II molecule shares the same nonasparagine polymorphism at position 57 of the β-chain as the diabetes-predisposing HLA-DQ8 (29). Therefore, we asked whether peripheral blood mononuclear cells from recent-onset diabetic children would recognize our panel of NOD-derived GFAP epitopes. As shown in Fig. 7, all three GFAP MHC class II peptides elicited proliferation at levels significantly different from healthy, autoantibody-negative FDRs. Notably, our I-A^{g7} GFAP216–230 epitope overlaps GFAP214–222, an epitope reported by Nepom and colleagues to bind HLA-A*0201 and induce granzyme B production in type 1 diabetic CTLs (28). This is consistent with other type 1 diabetes autoantigens where MHC class I and II epitopes have been found in overlapping regions or in close proximity (30,31).

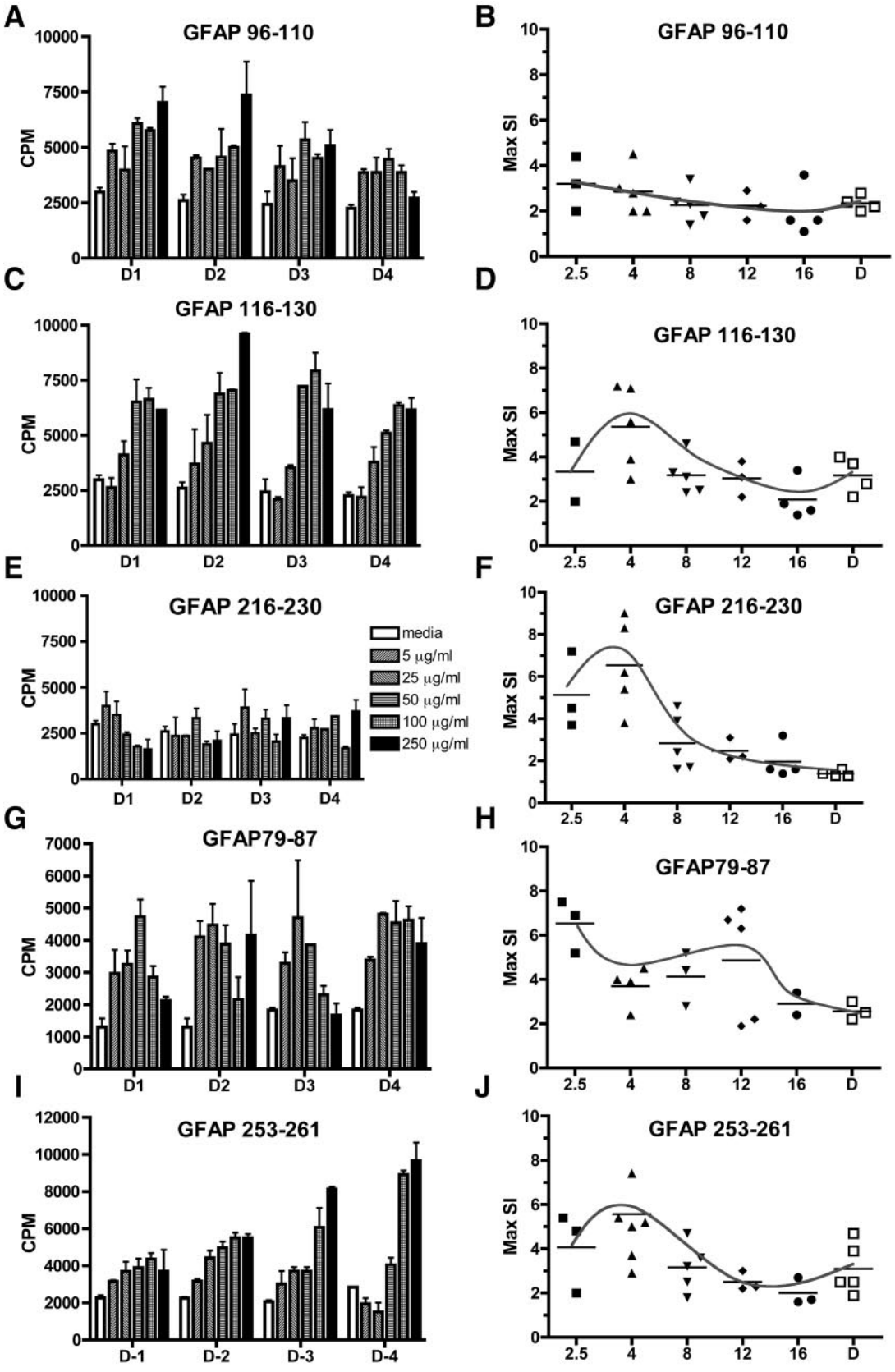

FIG. 5. Spontaneous T-cell responses to MHC Class I and Class II GFAP peptides in female NOD mice. Splenic T-cell proliferation to 15-mer I-A^{g7} GFAP peptides 96–110 (*A* and *B*), 116–130 (*C* and *D*), 216–230 (*E* and *F*), and 9-mer K^{d} peptides 79–87 (*G* and *H*), and 253–261 (*I* and *J*). Cpm results from four diabetic mice are plotted in the left column (*A*, *C*, *E*, *G*, and *I*), with media-normalized kinetic results from NOD females aged 2.5, 4, 8, 12, and 16 weeks or diabetic mice on the right (*B*, *D*, *F*, *H*, and *J*). Only the maximum SI value from 5–250 μg/ml peptide is shown. Red curve is for illustrative purposes only. Media values ranged from 208 to 2,985.

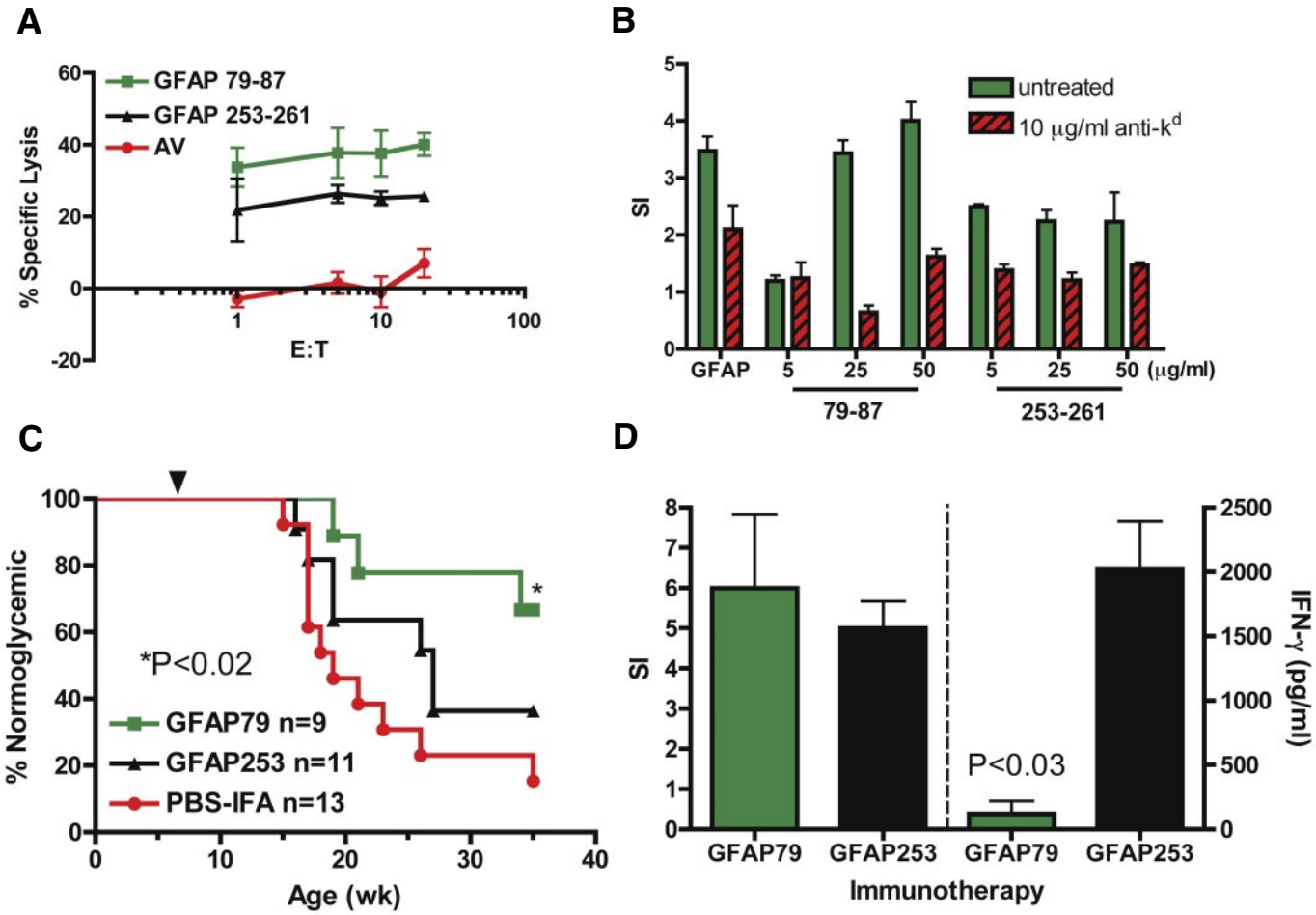

FIG. 6. Confirmation of GFAP 79–87 and 253–261 as CD8$^+$ T-cell epitopes and type 1 diabetes intervention. *A*: 8-week-old NOD females were immunized with 50 μg GFAP 79–87 or 253–261 in CFA and CD8$^+$ T-cells from draining lymph nodes harvested 5 days later for a ^{51}Cr release assay against peptide pulsed RMA-S(K^d) targets. The D^b binding AV peptide was used as negative control. *B*: Spontaneous splenic proliferative responses to GFAP 79–87 and 253–261 in 4-week-old NOD females were inhibited by 10 μg/ml anti-K^d antibody. Proliferation plotted as SI, with media range 248–444 cpm. Data are representative of two independent experiments. *C*: 8-week-old NOD females were immunized intraperitoneally with 100 μg GFAP 79–87 or 253–261 or vehicle emulsified in IFA (arrow). Immunotherapy with GFAP 79–87 significantly protected NOD mice from diabetes ($P < 0.02$, vs. PBS-IFA, log-rank analysis). *D*: Proliferative responses (left axis) by splenic T-cells to whole GFAP in nondiabetic GFAP 79-IFA – and GFAP 253–treated mice. Plotted as SI, media range 550-2929 cpm; $n = 3$ per group. IFN-γ production by splenocytes to whole-protein GFAP (*right axis*) ($n = 3$), measured by enzyme-linked immunosorbent assay. IFN-γ results were significantly different ($P < 0.03$, t test).

Although MHC class I genotyping was not performed in our patient set, MHC class I alleles are in linkage disequilibrium with DR3/DR4, and it is plausible that our K^d mapped peptides also bind risk-conferring HLA-A or -B alleles (32,33). Indeed, our K^d epitope GFAP 253–261, but not GFAP 79–87, gave proliferative responses statistically distinguishable between patients and healthy FDRs ($P <$ 0.003, Mann-Whitney t test).

By analyzing T-cell responses to a broad array of self-antigens, an overall measure of T-cell reactivity can be derived (34). The T-cell score is defined as the number of positive (SI >1.5) proliferative responses to an array of type 1 diabetes–relevant test antigens/peptides (35). Using this system and an autoreactivity cutoff of T-cell score ≥3, all type 1 diabetic patients and 2 of 6 FDRs in this dataset can be considered autoreactive, with one borderline (Fig. 7*B*). Intriguingly, when considering global GFAP responses (whole protein and peptides), the three autoreactive FDRs generated 50% (8 of 16) GFAP responses above SI 1.5 (Fig. 7*C*). A prospective, large-scale, blinded study comparing diabetic subjects, FDRs, and normal control subjects is under way as part of the Trials to Reduce IDDM in the Genetically at Risk (TRIGR) diabetes prevention trial, with the goal of identifying autoimmune responses with disease-predictive value.

DISCUSSION

β-Cell destruction and subsequent insulin deficiency are responsible for the clinical symptoms associated with type 1 diabetes. Our finding that autoimmune islet destruction is not β-cell exclusive but includes pSC suggests that other islet constituents may also be involved in type 1 diabetes etiology (9). Here, we demonstrate that pSC autoimmunity involves cognate CD8$^+$ T-cell targeting of GFAP.

Cultured pSC lacked MHC class II expression; therefore, we concentrated on cognate CD8$^+$ T-cell interactions. pSC targets were lysed by ex vivo CD8$^+$ T-cells from diabetic NOD mice, and transgenic rescue of MHC class I expression in pSC of NOD.β2m$^{-/-}$ mice significantly accelerated adoptively transferred type 1 diabetes, providing evidence for disease relevance and an in vivo correlate for the

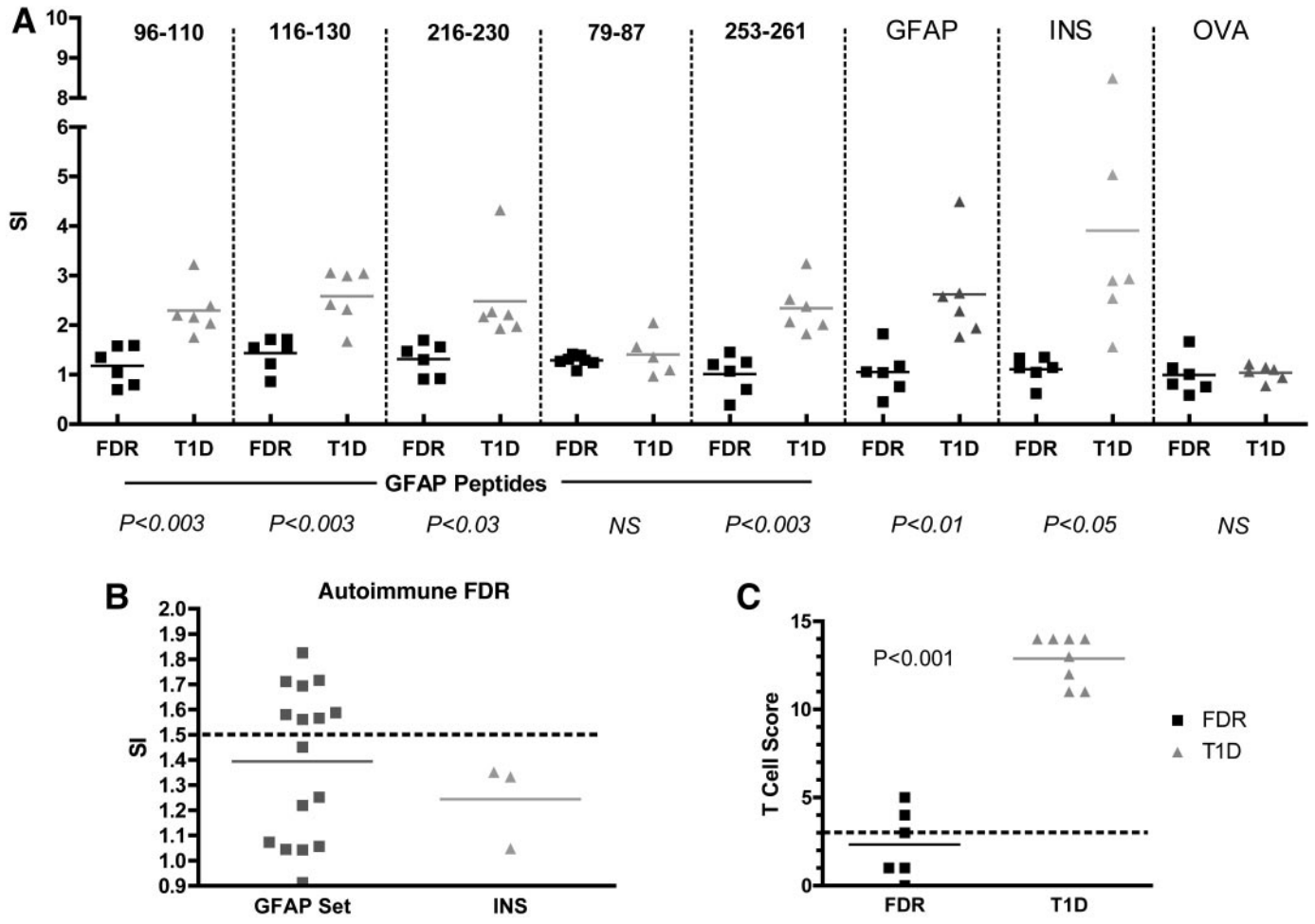

FIG. 7. Human T-cell responses to GFAP epitopes. *A*: peripheral blood mononuclear cells from recent-onset type 1 diabetics or FDRs were assayed. Shown are proliferative responses to 5 μg/ml GFAP peptides, whole GFAP, proinsulin, and ovalbumin (negative control). The GFAP peptides 96–110, 116–130, 216–230, and 253–261 elicited T-cell responses significantly different from those of FDRs (*P* values as shown, Mann-Whitney test). Media range 497–2242. *B*: T-cell autoreactivity plotted as T-cell score, representing the number of autoantigens with SI > 1.5. Autoreactivity cutoff placed at three (dotted line). *C*: Pan-GFAP response (protein and peptides) is presented for the three autoimmune FDRs compared with proinsulin. Dotted line at 1.5 SI.

cognate interaction observed between diabetogenic $CD8^+$ T-cells and pSCs in vitro. Here, hyperglycemia required 12–16 weeks while β-cells remained intact in MHC class I deficient animals, reinforcing the importance of $CD8^+$ T-cells in β-cell destruction (36).

This is the first report of primary pSC cultures facilitating molecular and functional studies of pSC, including their competence as antigen-presenting cells and association with and trophism for β-cells and relationship to peripheral glia. Physiologically, pSC loss may advance β-cell apoptosis by removal of neurotropic support, facilitating contact with pathogenic lymphocytes and disrupting islet architecture. Islet transplantation studies with or without pSC encapsulation and in combination with transgenic pSC modifications may be a new therapeutic strategy in type 1 diabetes.

GFAP was initially discovered as an autoantigen when analyzing brains from multiple sclerosis patients (10), which accumulate $GFAP^+$ astrocytes in the multiple sclerosis plaque. In response to injury, astrocytes synthesize GFAP in a process called astrogliosis (37,38); similarly, pSCs undergo gliosis following islet insult (39). We now extend our study of GFAP autoimmunity in type 1 diabetes from the protein to the peptide level, mapping three $I\text{-}A^{g7}$ and two K^d epitopes. Although we cannot rule out the presence of other GFAP epitopes, the MHC class I peptides 79–87 and 253–261 and the MHC class II peptides 96–110, 116–130, and 216–230 stimulated T-cell responses in nonimmunized NOD mice, diabetic children, and some FDRs. Confirmation of GFAP 106–120, revealed by CFA immunization, is under further investigation.

We employed immunotherapy to demonstrate disease relevance and were successful with GFAP 79–87. Although GFAP 253–261 was ineffective, immunotherapy depends on route, timing, and optimal dose for efficacy (22). Differences in affinity may account for the apparent disparity between the two K^d peptides. Mechanistically, GFAP 79–87 immunization nearly abolished IFN-γ production to whole-protein GFAP. Although IL-10 production remained equivalent, immunoregulation involving transforming growth factor-β is a likely explanation (40). Alterations in GFAP epitope targeting (Fig. S8) is another possibility.

GFAP autoimmunity may contribute to other type 1 diabetes–associated diseases such as multiple sclerosis, chronic inflammatory demyelinating polyradiculoneuropathy, (41) and Crohn's disease. We and others have shown a connection between type 1 diabetes and multiple scle-

rosis (5,6) and linkage between chronic inflammatory demyelinating polyradiculoneuropathy and type 1 diabetes (42,43) and Crohn's and type 1 diabetes (44,45) have been reported. Whether glial cells are generally involved in organ-selective autoimmunity remains to be determined.

The identification of GFAP epitopes is a crucial step in the development of GFAP tetramers and TCR transgenics. Why widely expressed neuronal autoantigens such as GFAP contribute to local islet inflammation remains unknown. Differences in tissue access, antigen processing and presentation, costimulation, and regulatory T-cell populations might, in combination, explain the islet selectivity of type 1 diabetes infiltrates (7,46,47). Genetic ablation of B7-2 induces a $CD4^+$ T-cell–mediated peripheral neuropathy, which presumably also targets GFAP, but with effector mechanisms distinct from those involved in type 1 diabetes (48). Whether the same GFAP peptides are targeted in B7-2–deficient NOD mice will be interesting to discern.

Recently, we have shown that sensory neurons are involved in a local regulatory circuit that controls islet inflammation and β-cell stress (4). Clearly, neuronal elements are involved in β-cell demise, and a complete understanding of type 1 diabetes pathogenesis will require a collaborative perspective between immunology and neuroscience.

ACKNOWLEDGMENTS

H.T. received scholarships from RESTRACOMP (Hospital for Sick Children), the Banting and Best Diabetes Centre, and the OGS Trust Fund. This research was supported by the Canadian Institutes for Health Research (CIHR) (to J.R.E., D.J.B., P.S.O., and H.-M.D.); by a University-Industry grant from CIHR and SynX Pharma, Toronto (to H.-M.D.); and by the Juvenile Diabetes Research Foundation, the National Institutes of Health (GCRC MO1 RR00084 and RO1 DK24021 to D.J.B.), and the Renziehausen fund (to D.J.B.).

We thank Lily Morikawa for histology and Drs. David Serreze, Pere Santamaria, and Michael Brenner for reagents.

REFERENCES

1. Anderson MS, Bluestone JA: The NOD mouse: a model of immune dysregulation. *Annu Rev Immunol* 23:447–485, 2005
2. Mathis D, Vence L, Benoist C: β-Cell death during progression to diabetes. *Nature* 414:792–798, 2001
3. Lieberman SM, DiLorenzo TP: A comprehensive guide to antibody and T-cell responses in type 1 diabetes . *Tissue Antigens* 62:359–377, 2003
4. Razavi R, Chan Y, Afifiyan F, Liu XJ, Wan X, Yantha J, Tsui H, Tang L, Tsai S, Santamaria P, Serreze D, Salter MW, Dosch H: $TRPV1^+$ sensory neurons control β cell stress and islet inflammation in autoimmune diabetes. *Cell* 127:1–13, 2006
5. Winer S, Astsaturov I, Cheung R, Gunaratnam L, Kubiak V, Cortez MA, Moscarello M, O'Connor PW, McKerlie C, Becker DJ, Dosch HM: Type I diabetes and multiple sclerosis patients target islet plus central nervous system autoantigens; nonimmunized nonobese diabetic mice can develop autoimmune encephalitis. *J Immunol* 166:2831–2841, 2001
6. Marrosu MG, Cocco E, Lai M, Spinicci G, Pischedda MP, Contu P: Patients with multiple sclerosis and risk of type 1 diabetes mellitus in Sardinia, Italy: a cohort study. *Lancet* 359:1461–1465, 2002
7. Salomon B, Rhee L, Bour-Jordan H, Hsin H, Montag A, Soliven B, Arcella J, Girvin AM, Padilla J, Miller SD, Bluestone JA: Development of spontaneous autoimmune peripheral polyneuropathy in B7–2-deficient NOD mice. *J Exp Med* 194:677–684, 2001
8. Setoguchi R, Hori S, Takahashi T, Sakaguchi S: Homeostatic maintenance of natural Foxp3(+) CD25(+) CD4(+) regulatory T-cells by interleukin (IL)-2 and induction of autoimmune disease by IL-2 neutralization. *J Exp Med* 201:723–735, 2005
9. Winer S, Tsui H, Lau A, Song A, Li X, Cheung RK, Sampson A, Afifiyan F, Elford A, Jackowski G, Becker DJ, Santamaria P, Ohashi P, Dosch HM: Autoimmune islet destruction in spontaneous type 1 diabetes is not beta-cell exclusive. *Nat Med* 9:198–205, 2003
10. Eng LF, Ghirnikar RS, Lee YL: Glial fibrillary acidic protein: GFAP-thirty-one years (1969–2000). *Neurochem Res* 25:1439–1451, 2000
11. Carrillo J, Puertas MC, Alba A, Ampudia RM, Pastor X, Planas R, Riutort N, Alonso N, Pujol-Borrell R, Santamaria P, Vives-Pi M, Verdaguer J: Islet-infiltrating B-cells in nonobese diabetic mice predominantly target nervous system elements. *Diabetes* 54:69–77, 2005
12. Brenner M, Messing A: GFAP transgenic mice. *Methods* 10:351–364, 1996
13. Lewis SA, Balcarek JM, Krek V, Shelanski M, Cowan NJ: Sequence of a cDNA clone encoding mouse glial fibrillary acidic protein: structural conservation of intermediate filaments. *Proc Natl Acad Sci U S A* 81:2743–2746, 1984
14. MacDonald PE, Sewing S, Wang J, Joseph JW, Smukler SR, Sakellaropoulos G, Saleh MC, Chan CB, Tsushima RG, Salapatek AM, Wheeler MB: Inhibition of Kv2.1 voltage-dependent K+ channels in pancreatic beta-cells enhances glucose-dependent insulin secretion. *J Biol Chem* 277:44938–44945, 2002
15. Vroemen M, Weidner N: Purification of Schwann cells by selection of p75 low affinity nerve growth factor receptor expressing cells from adult peripheral nerve. *J Neurosci Methods* 124:135–143, 2003
16. Han B, Serra P, Amrani A, Yamanouchi J, Maree AF, Edelstein-Keshet L, Santamaria P: Prevention of diabetes by manipulation of anti-IGRP autoimmunity: high efficiency of a low-affinity peptide. *Nat Med* 11:645–652, 2005
17. Portis AJ, Rajotte RV, Krukoff TL: Reinnervation of isolated islets of Langerhans transplanted beneath the kidney capsule in the rat. *Cell Transplant* 3:163–170, 1994
18. Tsuyuki Y, Fujimaki H, Hikawa N, Fujita K, Nagata T, Minami M: IFN-gamma induces coordinate expression of MHC class I-mediated antigen presentation machinery molecules in adult mouse Schwann cells. *Neuroreport* 9:2071–2075, 1998
19. Wicker LS, Leiter EH, Todd JA, Renjilian RJ, Peterson E, Fischer PA, Podolin PL, Zijlstra M, Jaenisch R, Peterson LB: β2-microglobulin–deficient NOD mice do not develop insulitis or diabetes. *Diabetes* 43:500–504, 1994
20. Serreze DV, Leiter EH, Christianson GJ, Greiner D, Roopenian DC: Major histocompatibility complex class I–deficient NOD-*B2*m^{null} mice are diabetes and insulitis resistant. *Diabetes* 43:505–509, 1994
21. Serreze DV, Chapman HD, Varnum DS, Gerling I, Leiter EH, Shultz LD: Initiation of autoimmune diabetes in NOD/Lt mice is MHC class I-dependent. *J Immunol* 158:3978–3986, 1997
22. Winer S, Gunaratnam L, Astsatourov I, Cheung RK, Kubiak V, Karges W, Hammond-McKibben D, Gaedigk R, Graziano D, Trucco M, Becker DJ, Dosch HM: Peptide dose, MHC affinity, and target self-antigen expression are critical for effective immunotherapy of nonobese diabetic mouse prediabetes. *J Immunol* 165:4086–4094, 2000
23. Lieberman SM, Takaki T, Han B, Santamaria P, Serreze DV, DiLorenzo TP: Individual nonobese diabetic mice exhibit unique patterns of CD8+ T-cell reactivity to three islet antigens, including the newly identified widely expressed dystrophia myotonica kinase. *J Immunol* 173:6727–6734, 2004
24. Graser RT, DiLorenzo TP, Wang F, Christianson GJ, Chapman HD, Roopenian DC, Nathenson SG, Serreze DV: Identification of a CD8 T-cell that can independently mediate autoimmune diabetes development in the complete absence of CD4 T-cell helper functions. *J Immunol* 164:3913–3918, 2000
25. Chen YG, Choisy-Rossi CM, Holl TM, Chapman HD, Besra GS, Porcelli SA, Shaffer DJ, Roopenian D, Wilson SB, Serreze DV: Activated NKT-cells inhibit autoimmune diabetes through tolerogenic recruitment of dendritic cells to pancreatic lymph nodes. *J Immunol* 174:1196–1204, 2005
26. Harrison LC, Honeyman MC, Trembleau S, Gregori S, Gallazzi F, Augstein P, Brusic V, Hammer J, Adorini L: A peptide-binding motif for I-A(g7), the class II major histocompatibility complex (MHC) molecule of NOD and Biozzi AB/H mice. *J Exp Med* 185:1013–1021, 1997
27. Gregori S, Bono E, Gallazzi F, Hammer J, Harrison LC, Adorini L: The motif for peptide binding to the insulin-dependent diabetes mellitus-associated class II MHC molecule I-Ag7 validated by phage display library. *Int Immunol* 12:493–503, 2000
28. Standifer NE, Ouyang Q, Panagiotopoulos C, Verchere CB, Tan R, Greenbaum CJ, Pihoker C, Nepom GT: Identification of novel HLA-A*0201–restricted epitopes in recent-onset type 1 diabetic subjects and antibody-positive relatives. *Diabetes* 55:3061–3067, 2006
29. Dorman JS, Bunker CH: HLA-DQ locus of the human leukocyte antigen complex and type 1 diabetes mellitus: a HuGE review. *Epidemiol Rev* 22:218–227, 2000

30. Wong FS, Karttunen J, Dumont C, Wen L, Visintin I, Pilip IM, Shastri N, Pamer EG, Janeway CA Jr: Identification of an MHC class I-restricted autoantigen in type 1 diabetes by screening an organ-specific cDNA library. *Nat Med* 5:1026–1031, 1999
31. Mukherjee R, Wagar D, Stephens TA, Lee-Chan E, Singh B: Identification of CD4+ T-cell-specific epitopes of islet-specific glucose-6-phosphatase catalytic subunit-related protein: a novel {beta} cell autoantigen in type 1 diabetes. *J Immunol* 174:5306–5315, 2005
32. Valdes AM, Erlich HA, Noble JA: Human leukocyte antigen class I B and C loci contribute to type 1 diabetes (T1D) susceptibility and age at type 1 diabetes onset. *Hum Immunol* 66:301–313, 2005
33. Noble JA, Valdes AM, Bugawan TL, Apple RJ, Thomson G, Erlich HA: The HLA class I A locus affects susceptibility to type 1 diabetes. *Hum Immunol* 63:657–664, 2002
34. Dosch H, Cheung RK, Karges W, Pietropaolo M, Becker DJ: Persistent T-cell anergy in human type 1 diabetes. *J Immunol* 163:6933–6940, 1999
35. Seyfert-Margolis V, Gisler TD, Asare AL, Wang RS, Dosch HM, Brooks-Worrell B, Eisenbarth GS, Palmer JP, Greenbaum CJ, Gitelman SE, Nepom GT, Bluestone JA, Herold KC: Analysis of T-cell assays to measure autoimmune responses in subjects with type 1 diabetes: results of a blinded controlled study. *Diabetes* 55:2588–2594, 2006
36. Kay TW, Parker JL, Stephens LA, Thomas HE, Allison J: RIP-beta 2-microglobulin transgene expression restores insulitis, but not diabetes, in beta 2-microglobulin null nonobese diabetic mice. *J Immunol* 157:3688–3693, 1996
37. Eddleston M, Mucke L: Molecular profile of reactive astrocytes–implications for their role in neurologic disease. *Neuroscience* 54:15–36, 1993
38. Eng LF, Ghirnikar RS: GFAP and astrogliosis. *Brain Pathol* 4:229–237, 1994
39. Teitelman G, Guz Y, Ivkovic S, Ehrlich M: Islet injury induces neurotrophin expression in pancreatic cells and reactive gliosis of peri-islet Schwann cells. *J Neurobiol* 34:304–318, 1998
40. You S, Thieblemont N, Alyanakian MA, Bach JF, Chatenoud L: Transforming growth factor-beta and T-cell-mediated immunoregulation in the control of autoimmune diabetes. *Immunol Rev* 212:185–202, 2006
41. Koller H, Kieseier BC, Jander S, Hartung HP: Chronic inflammatory demyelinating polyneuropathy. *N Engl J Med* 352:1343–1356, 2005
42. Sharma KR, Cross J, Farronay O, Ayyar DR, Shebert RT, Bradley WG: Demyelinating neuropathy in diabetes mellitus. *Arch Neurol* 59:758–765, 2002
43. Fudge E, Carol J, She JX, Dosch M, Atkinson M, Muir A: Chronic inflammatory demyelinating polyradiculoneuropathy in two children with type 1 diabetes mellitus. *Pediatr Diabetes* 6:244–248, 2005
44. Dorman JS, Steenkiste AR, O'Leary LA, McCarthy BJ, Lorenzen T, Foley TP: Type 1 diabetes in offspring of parents with type 1 diabetes: the tip of an autoimmune iceberg? *Pediatr Diabetes* 1:17–22, 2000
45. Sipetic S, Vlajinac H, Kocev N, Marinkovic J, Radmanovic S, Denic L: Family history and risk of type 1 diabetes mellitus. *Acta Diabetol* 39:111–115, 2002
46. O'Brien BA, Huang Y, Geng X, Dutz JP, Finegood DT: Phagocytosis of apoptotic cells by macrophages from NOD mice is reduced. *Diabetes* 51:2481–2488, 2002
47. Alyanakian MA, You S, Damotte D, Gouarin C, Esling A, Garcia C, Havouis S, Chatenoud L, Bach JF: Diversity of regulatory CD4+T-cells controlling distinct organ-specific autoimmune diseases. *Proc Natl Acad Sci U S A* 100:15806–15811, 2003
48. Bour-Jordan H, Thompson HL, Bluestone JA: Distinct effector mechanisms in the development of autoimmune neuropathy versus diabetes in nonobese diabetic mice. *J Immunol* 175:5649–5655, 2005